



## OPEN Enzyme assisted carbon dioxide capture and mineralization in construction relevant alkaline materials

Nabeel Liaqat & Xiong Bill Yu

Mineralizing CO<sub>2</sub> in alkaline construction materials can reduce process emissions. This study measures the effect of carbonic anhydrase on CO<sub>2</sub> uptake and retention in hydrated lime, Portland cement, fly ash, and slag under ambient conditions using a mass-flow-controlled CO<sub>2</sub> supply and gravimetric tracking. CO<sub>2</sub> was supplied for 1440 min for hydrated lime and cement and for 360 min for fly ash and slag, then stopped to quantify permanently retained mass. Carbonic anhydrase increased total CO<sub>2</sub> uptake across all materials by 71 to 89 percent. Hydrated lime reached 474.1 mg g<sup>-1</sup> with the enzyme. Cement reached 285.9 mg g<sup>-1</sup>. Fly ash and slag reached 308.3 mg g<sup>-1</sup> and 312.4 mg g<sup>-1</sup>. The fraction retained after cutoff increased for all solids and was nearly complete in several enzyme cases, while water controls showed negligible permanence. Enzyme reuse over four cycles retained 87.9 percent of the initial performance. The data support a surface-coupled mechanism in which the enzyme accelerates CO<sub>2</sub> hydration in the particle boundary layer, increases local carbonate availability, and drives precipitation with Ca<sup>2+</sup> and Mg<sup>2+</sup> on solid surfaces. The reaction endpoint remains unchanged; only the rate is altered. These results define material-enzyme combinations and operating conditions for enzyme-assisted mineralization in construction-relevant systems.

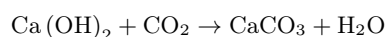
**Keywords** Climate change, Sustainable engineering, Carbonic anhydrase, Carbon sequestration, CO<sub>2</sub> mineralization, Enzyme reuse, Biocatalysis, Waste valorization

Global climate change is an important issue that requires immediate action. The increasing content of greenhouse gases in the air, including carbon dioxide, is believed to be a major cause of global climate change. For example, as of August 2025, the amount of CO<sub>2</sub> in the air, as recorded by NOAA at Mauna Loa Observatory in Hawaii, reached 425.48 ppm, up from 317.45 ppm in April 1958. Human activities such as construction, burning fossil fuels, deforestation, and industrial processes are the major sources of anthropogenic CO<sub>2</sub><sup>1</sup>.

Carbon dioxide capture technology is employed to reduce CO<sub>2</sub> emissions, which sees rapid advancement driven by the emergence of new approaches that are designed to more effectively and efficiently trap and store CO<sub>2</sub> emissions<sup>2,3</sup>. CO<sub>2</sub> Capture, Utilization and Storage (CCUS) has gained significant attention in recent years to reduce CO<sub>2</sub> emissions. CCUS entails the collection of carbon dioxide emissions from diverse sources, such as power plants or industrial sites. The captured CO<sub>2</sub> is subsequently either utilized or stored<sup>4,5</sup>.

The construction industry contributes significantly to global anthropogenic CO<sub>2</sub> emissions. The Global Alliance for Buildings & Construction (GlobalABC) and United Nations Environment Programme (UNEP), in their 2024/2025 Global Status Report for Buildings and Construction, report that the sector is responsible for about 34% of global CO<sub>2</sub> emissions and approximately 32% of global final energy consumption. Therefore, reducing CO<sub>2</sub> emissions associated with construction is essential to help mitigate the effects of climate change<sup>6,7</sup>.

CO<sub>2</sub> absorption and fixation with alkaline materials presents a major opportunity due to their high pH and abundance of reactive cations such as Ca<sup>2+</sup> and Mg<sup>2+</sup>. Under alkaline conditions, dissolved CO<sub>2</sub> undergoes hydration to form bicarbonate (HCO<sub>3</sub><sup>-</sup>) and carbonate (CO<sub>3</sub><sup>2-</sup>) ions, which readily react with these cations to produce stable carbonate minerals such as CaCO<sub>3</sub> and MgCO<sub>3</sub>. For example, the calcium hydrate produced by cement hydration provides a sink for CO<sub>2</sub><sup>8,9</sup>.

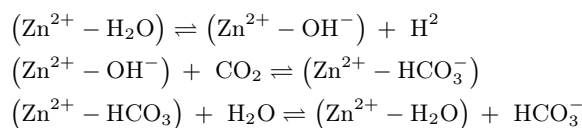


Department of Civil and Environmental Engineering, Case Western Reserve University, 2104 Adelbert Road, Cleveland, OH 44106-720, USA. email: xxy21@case.edu

The high alkalinity accelerates these reactions by shifting the equilibrium toward carbonate formation, thereby enhancing the permanent sequestration of CO<sub>2</sub> in the form of thermodynamically stable mineral phases. For example, the calcium hydroxide produced during cement hydration serves as an efficient sink for CO<sub>2</sub> through the carbonation of portlandite to calcite, improving both environmental sustainability and material durability<sup>10,11</sup>. Also, a significant amount of alkaline waste is produced annually, such as fly ash, slag. Carbonation of this alkaline waste provides a major pathway for CO<sub>2</sub> absorption and improves the properties when used for cement and concrete production<sup>12</sup>. Enzyme-based CO<sub>2</sub> capture technologies offer promising opportunities for greener industrial processes and materials. Enzymes, naturally occurring catalysts in living organisms, are highly efficient, with reaction rates often enhanced by factors of 10<sup>6</sup> to 10<sup>12</sup> compared to inorganic catalysts<sup>13</sup>.

The CO<sub>2</sub> absorption capacity of cement can be significantly enhanced by incorporating industrial byproducts and enzymes. Cement and enzymes not only contribute to reducing carbon dioxide (CO<sub>2</sub>) emissions during manufacturing but also actively absorb CO<sub>2</sub> from the environment over time<sup>14,15</sup>. The combination of industrial byproducts and enzyme-enriched cement holds great potential for minimizing carbon emissions in the construction industry while facilitating environmental CO<sub>2</sub> absorption. Such approaches align with sustainable development goals and contribute to mitigating climate change<sup>16,17</sup>.

The carbonic anhydrase (CA) enzyme has garnered significant attention for its exceptional catalytic efficiency and ability to function under moderate environmental conditions, making it ideal for CO<sub>2</sub> capture technologies. Carbonic anhydrases are primarily zinc-containing enzymes distributed across prokaryotes, eukaryotes, and extremophiles. These enzymes are metalloenzymes grouped into at least eight classes, α, β, γ, δ, ζ, η, θ, and ι, which differ in fold and active-site architecture yet catalyze the same reversible CO<sub>2</sub> hydration reaction. The η class was identified in *Plasmodium* spp., θ in marine diatoms, and the most recently described ι class occurs in both diatoms and bacteria<sup>18,19</sup>. However, all CA classes share a uniform catalytic mechanism, converting CO<sub>2</sub> into bicarbonate and a proton through reversible hydration and dehydration reactions, as shown in the equations below<sup>20–22</sup>.



Carbonic anhydrase plays a critical role in various biological processes, including CO<sub>2</sub> transport, pH regulation, cell respiration, and photosynthesis<sup>23,24</sup>. Its ability to catalyze the reversible hydration of CO<sub>2</sub>, even under conditions found in industrial flue gases, has opened new avenues for biomimetic CO<sub>2</sub> sequestration. This process, which mimics biological CO<sub>2</sub> capture mechanisms, has shown promising results in capturing CO<sub>2</sub> from industrial processes<sup>25</sup>. CA's remarkable turnover rate of up to 10<sup>4</sup>–10<sup>7</sup> s<sup>-1</sup> makes it highly efficient for these applications<sup>23</sup>.

Carbon capture and storage (CCS) is an effective strategy for achieving carbon neutrality by improving carbon capture efficiency. Recognized by the International Energy Agency, CCS enables the development of net-zero energy emission systems, supporting global efforts to combat climate change<sup>26</sup>.

The rationale for selecting materials such as cement, lime, fly ash, and slag lies in their widespread availability and industrial significance. Cement is a major construction material with considerable CO<sub>2</sub> emissions during production, while lime, fly ash, and slag are common industrial byproducts that present disposal and environmental challenges<sup>27,28</sup>. Investigating the CO<sub>2</sub> absorption capabilities of these materials allows for identifying effective carbon capture methods while promoting sustainable uses for industrial byproducts, addressing both environmental and waste management issues.

Previous studies have established carbonic anhydrase as a highly efficient biocatalyst for accelerating the reversible hydration of carbon dioxide in aqueous systems, gas–liquid membrane contactors, and bio-based capture processes. However, most existing research has concentrated on controlled laboratories or biological environments, with limited exploration of CA's interaction with complex solid–liquid matrices such as industrial alkaline waste. These materials, rich in calcium and magnesium oxides, offer natural potential for CO<sub>2</sub> mineralization but are often limited by slow reaction kinetics and surface diffusion barriers under ambient conditions<sup>23,29,30</sup>. The integration of CA into such heterogeneous systems remains largely unexplored, particularly in the context of construction-related materials like hydrated lime, fly ash, slag, and cement. This study addresses this research gap by systematically quantifying the catalytic effect of CA on CO<sub>2</sub> absorption and mineralization across these materials, thereby providing new mechanistic insights and experimental evidence for enzyme-assisted carbon capture using readily available industrial byproducts<sup>31–33</sup>.

This study quantifies how carbonic anhydrase (CA) alters both the kinetics and permanence of CO<sub>2</sub> uptake in alkaline industrial materials, hydrated lime, Portland cement, fly ash, and slag, tested under ambient laboratory conditions using a controlled gas-delivery and gravimetric protocol. Specifically, we measure total CO<sub>2</sub> uptake per unit mass during continuous CO<sub>2</sub> exposure, and we determine permanent uptake as the mass retained after CO<sub>2</sub> cutoff and a defined stabilization window, thereby separating reversible dissolution from mineral fixation. We compare CA-treated and control samples to assess initial uptake rates and time to 90% of peak (t<sub>90</sub>), and we rank materials by peak uptake, permanent uptake, and retention fraction to identify top-performing CA-material combinations. We also evaluate enzyme reusability over four consecutive cycles using hydrated lime as a reference substrate and test statistical significance with triplicate measurements per condition (one-way ANOVA and two-sample t-tests at α = 0.05). Our working hypothesis is that CA, acting as a kinetic accelerator of CO<sub>2</sub> hydration, increases both peak and permanent uptake, with the magnitude of benefit scaling with available alkaline earth cations (Ca<sup>2+</sup>/Mg<sup>2+</sup>) and baseline alkalinity. A detailed description of the gas-delivery setup, timing of exposure, post-cutoff stabilization, and data-analysis procedures is provided in Materials and Methods.

## Experimental materials and methodology

### Experimental materials

The materials used in this study include carbonic anhydrase enzyme, hydrated lime, fly ash, slag, cement, deionized water, and a CO<sub>2</sub> gas cylinder. Research-grade carbonic anhydrase was procured from Sigma-Aldrich in the form of lyophilized powder. The CA used in this study belongs to the  $\alpha$ -class of carbonic anhydrases, extracted from bovine erythrocytes, which are known for their high turnover rate (up to 10<sup>6</sup> s<sup>-1</sup>), pH stability in the range of 6.5–10, and temperature stability up to 60 °C. These properties make  $\alpha$ -CA a robust and well-characterized model enzyme for laboratory-scale CO<sub>2</sub> capture systems. Hydrated lime, specifically autoclaved mason's lime, was obtained from Graymont, Inc. with a pH value of 12.1 in a 10% aqueous solution. Fly ash and slag were both sourced from Rockport Ready Mix Inc., Cleveland, Ohio, USA, with pH values of 10.2 and 10.7, respectively, when dispersed in DI water. Portland cement (Type I/II or IL) was purchased from Home Depot with a pH value of 12.4 in aqueous suspension. The CO<sub>2</sub> gas cylinder used in the experiments was procured from AIRGAS. Deionized water was used throughout all experiments.

### Preparation of carbonic anhydrase solution

To prepare the carbonic anhydrase (CA) solution, 2.7 mg of the powdered enzyme was accurately weighed and dissolved in 1 mL of deionized water, resulting in a working concentration of 2.7 mg/mL ( $\geq 2,000$  W-A units/mg protein). This concentration was selected based on preliminary optimization trials and previous studies demonstrating that enzyme activities above  $\sim 2$  mg/mL achieve a balance between catalytic efficiency and cost-effectiveness for CO<sub>2</sub> hydration reactions under ambient conditions<sup>34,35</sup>. The same enzyme concentration and preparation protocol were maintained across all experiments to ensure consistency and reproducibility of results.

### Experimental setup

CO<sub>2</sub> and N<sub>2</sub> gas cylinders were procured from Airgas and used as gas sources for the experiment. Each cylinder was connected to a low-pressure regulator to maintain a safe and controlled pressure level. The regulated gas lines were connected to mass flow controllers (MFCs) from Alicat, model BASIS™ Series. These MEMS-based thermal mass flow controllers are designed for precise and compact flow regulation, offering a flow range from 100 SCCM to 100 SLPM, operating pressure up to 145 PSIG, 1,000:1 turndown ratio. The gas streams from the MFCs were directed into a mixing chamber, allowing adjustment of gas composition when needed. After the mixing chamber, the gas stream was passed through a flow meter from Kelly Pneumatics to verify the flow rate<sup>36,37</sup>. This flow meter supports flow accuracy of  $\pm 2\%$  of reading or 0.05 SLPM, a flow range up to 200 SLPM, a sample rate of 50 ms, and an operating temperature of 0–50 °C. Following the flow meter, the gas line included a particulate filter to remove solid particles, a water trap to prevent moisture from entering the sample vial, and a hydrophobic filter to block water vapor from contaminating the gas stream. All filters used in the system were procured from CO2Meter<sup>38,39</sup>. The gas was then delivered through a fine needle into a sealed 2 mL airtight glass sampling tube, which contained the test material. The sampling tube was placed on a high-precision analytical balance capable of measuring mass changes up to four decimal places ( $\pm 0.0001$  g accuracy). During the experiment, CO<sub>2</sub> gas was supplied at a constant pressure of 1 bar, and the change in weight of the sampling tube was recorded over time to monitor the amount of CO<sub>2</sub> absorbed. After a set period, the CO<sub>2</sub> supply was stopped at 1440 min for hydrated lime and cement, and at 360 min for fly ash and slag, when the uptake curve reached an apparent equilibrium, and the balance continued recording to determine the amount of CO<sub>2</sub> permanently retained. All samples were prepared to maintain a consistent total mass of 1.5 g, including solid and water, ensuring uniformity across tests. The samples were prepared such that the total weight, including both the solid and liquid components, was maintained at 1.5 g to ensure consistency across all experimental conditions throughout the study. The complete experimental setup is shown in Fig. 1.

## Results and discussion

### Material characterization

#### Lime

The microstructural and elemental characteristics of hydrated lime were analyzed using SEM and EDS. Figure 3a shows that calcium (Ca) and oxygen (O) are the dominant elements, with strong peaks at  $\sim 3.7$  keV, 4.0 keV (Ca), and 0.5 keV (O). Carbon (C) was also present, likely due to partial carbonation. Minor peaks for Mg, Al, Si, K, and Fe indicate trace impurities. EDS data Fig. 2 confirms CaO as the primary component (94.01 wt.%), consistent with Ca(OH)<sub>2</sub>, along with minor oxides like MgO, Al<sub>2</sub>O<sub>3</sub>, and SiO<sub>2</sub>. The SEM image in Fig. 3b reveals a porous structure of jagged particles, providing a high surface area for CO<sub>2</sub> interaction. These properties support lime's suitability for enzyme-enhanced CO<sub>2</sub> mineralization.

#### Fly ash

The chemical composition and microstructure of fly ash were examined using EDS and SEM and are shown in Fig. 4. The EDS spectrum Fig. 4a shows dominant peaks for O, Si, and Al, indicating major oxides like SiO<sub>2</sub> and Al<sub>2</sub>O<sub>3</sub>, along with notable amounts of Ca, Fe, Mg, S, K, Na, Ti, and trace Ni. Figure 2 confirms its pozzolanic nature, with high SiO<sub>2</sub> (35.38 wt.%) and Al<sub>2</sub>O<sub>3</sub> (19.91 wt.%), and other oxides including CaO and FeO. The SEM image in Fig. 4b shows spherical particles (cenospheres) within an amorphous matrix, offering high surface area and porosity, favorable for CO<sub>2</sub> interaction and mineralization, especially under enzymatic enhancement.

#### Slag

The slag sample was analyzed using EDS and SEM to assess its composition and surface morphology. The EDS spectrum in Fig. 5a shows dominant peaks for Ca, Si, and O, along with Mg, Al, Fe, S, and trace elements like Na,

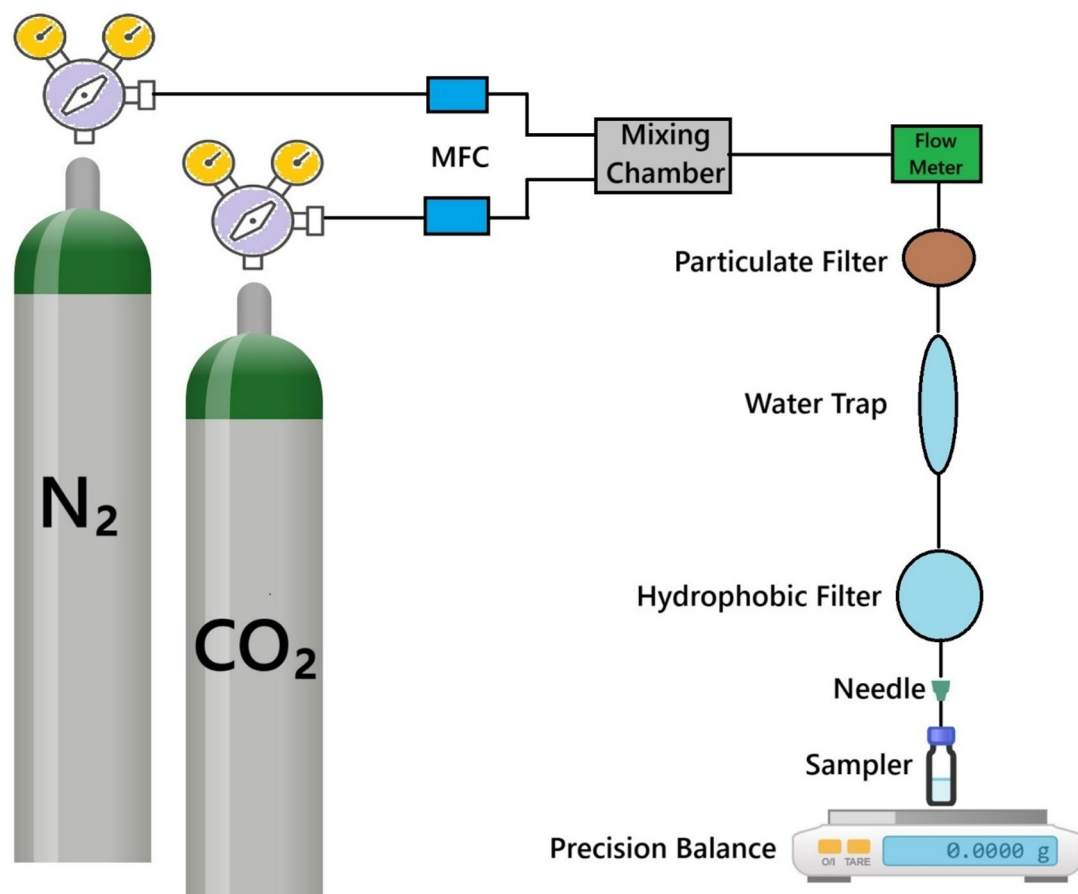


**Fig. 1.** Experimental setup For CO<sub>2</sub> absorption measurement.

K, Ti, and Mn, indicating a complex mineralogy typical of metallurgical slag. Figure 2 shows high CaO (39.16 wt.%) and SiO<sub>2</sub> (33.73 wt.%), followed by MgO and Al<sub>2</sub>O<sub>3</sub>. The SEM image in Fig. 5b shows angular, fractured particles with rough surfaces, providing increased surface area and nucleation sites. This dense microstructure favors stable CO<sub>2</sub> mineralization, especially under enzyme-catalyzed conditions.

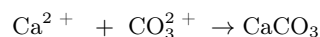
### Mechanism of CO<sub>2</sub> mineralization

Figure 6 presents a two-stage conceptual model illustrating the mechanism of carbonic anhydrase-assisted CO<sub>2</sub> capture and mineralization using alkaline industrial waste materials. In the first stage, carbon dioxide (CO<sub>2</sub>) gas diffuses into the aqueous phase, where it undergoes rapid hydration catalyzed by the enzyme carbonic anhydrase. This enzymatic reaction significantly accelerates the otherwise slow conversion of CO<sub>2</sub> and water into bicarbonate ions (HCO<sub>3</sub><sup>-</sup>) and protons (H<sup>+</sup>), as shown below:



This reaction increases the concentration of reactive bicarbonates in solution, forming the basis for subsequent mineralization.

In the second stage, calcium ions (Ca<sup>2+</sup>), released from alkaline materials such as hydrated lime, fly ash, or slag, react with bicarbonate to form carbonate ions (CO<sub>3</sub><sup>2-</sup>). These carbonate ions then combine with Ca<sup>2+</sup> to form solid calcium carbonate (CaCO<sub>3</sub>) precipitates:



This mineral precipitation pathway effectively sequesters CO<sub>2</sub> as a thermodynamically stable solid, enabling long-term carbon storage. The enzymatic enhancement ensures faster reaction kinetics and greater utilization of calcium-bearing waste materials, thereby improving the overall CO<sub>2</sub> capture efficiency.

### CO<sub>2</sub> absorption in alkaline systems

Figure 7 presents the CO<sub>2</sub> absorption behavior of pure water and enzyme solution (carbonic anhydrase dissolved in water) over a period of 7200 min. During the first 1440 min, CO<sub>2</sub> gas was continuously supplied. After this point, the gas flow was stopped to observe desorption behavior.

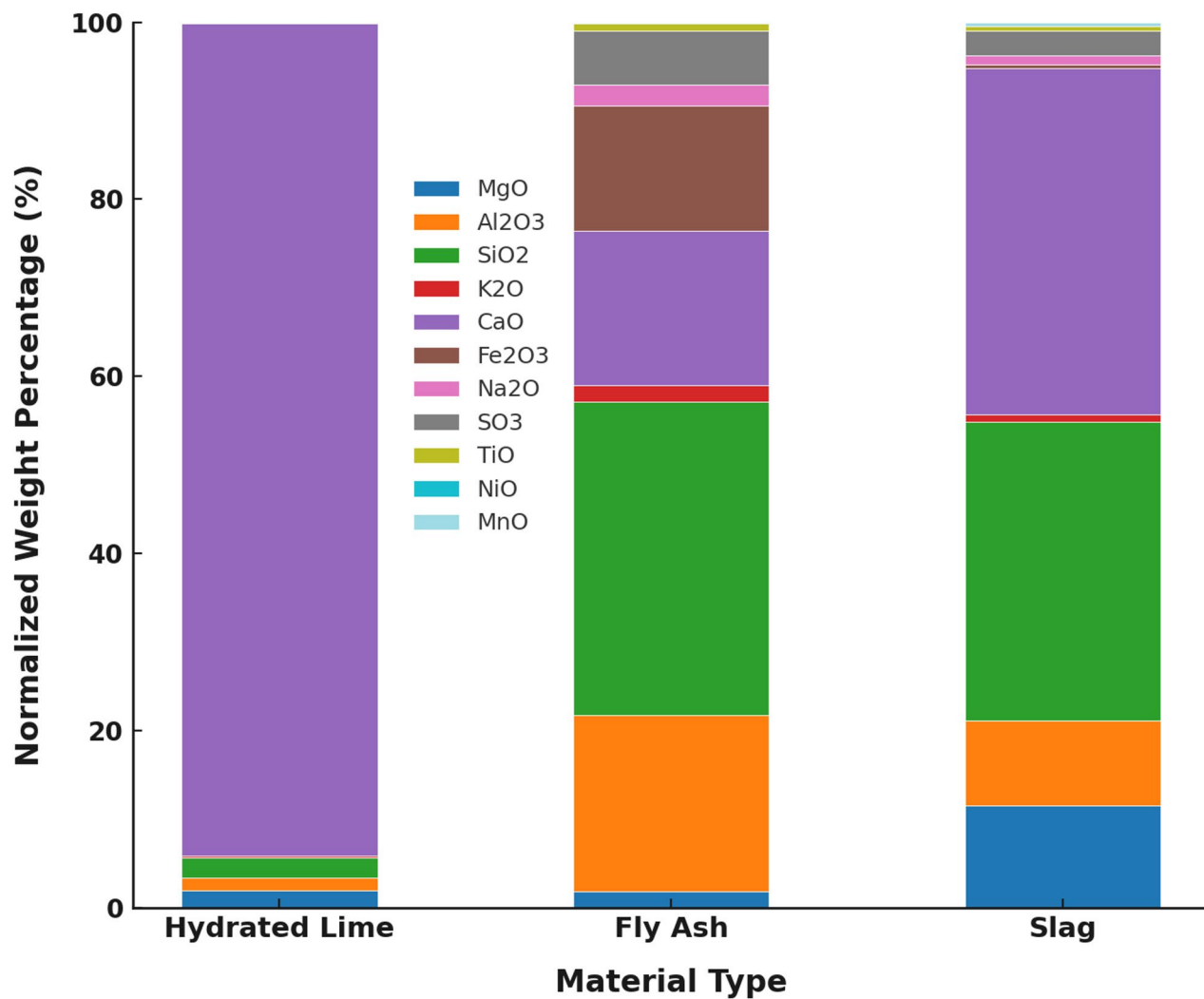


Fig. 2. Major oxides in hydrated lime, fly ash, and slag.

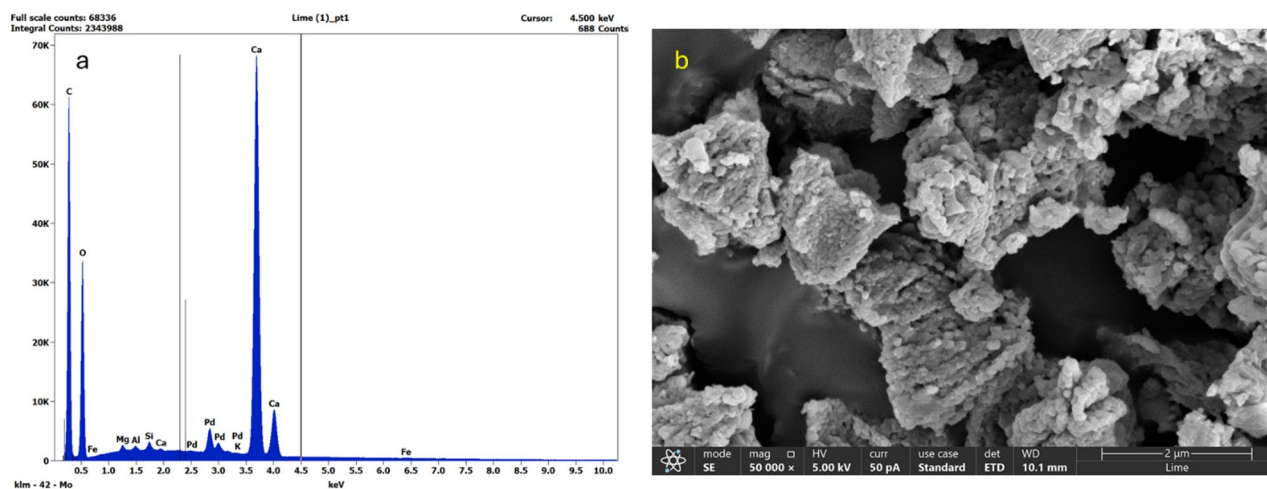
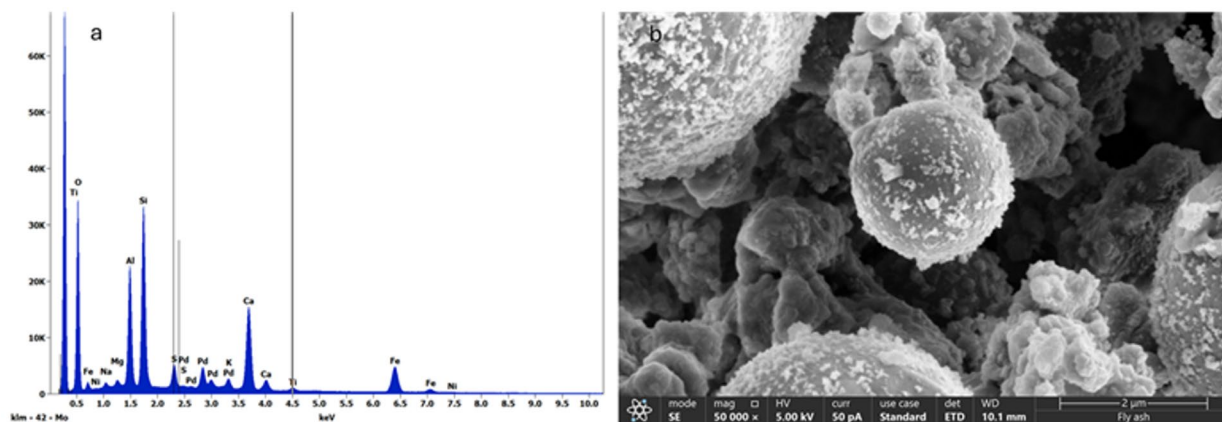
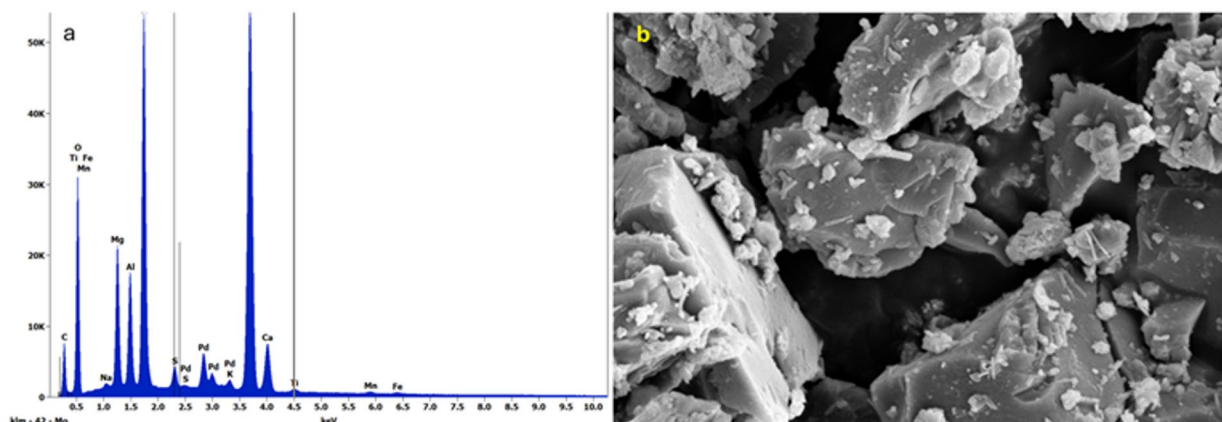


Fig. 3. (a) Eds spectrum showing calcium and oxygen as major elements in hydrated lime; (b) Sem image At 50,000× magnification displaying its porous, irregular surface.



**Fig. 4.** (a) EDS spectrum showing major elements in fly ash, including Si, Al, O, Ca, and Fe; (b) SEM image at 50,000 $\times$  magnification showing spherical and irregular particle morphology.



**Fig. 5.** (a) EDS spectrum of slag showing major peaks for Ca, Si, O, and Mg; (b) SEM image at 50,000 $\times$  magnification showing angular and fractured particle surfaces favorable for CO<sub>2</sub> mineralization.

In the case of water, a slight initial decrease in mass occurred, likely due to water evaporation. This was followed by a gradual increase in CO<sub>2</sub> absorption, reaching a peak value of approximately 239.53 mg/g at 1440 min. Once the CO<sub>2</sub> supply was cut off, the absorbed gas was gradually released, and the mass returned close to its original value by 2880 min, indicating nearly complete desorption of CO<sub>2</sub>.

In contrast, the enzyme solution exhibited a significantly faster and higher CO<sub>2</sub> absorption rate. A rapid mass increase was recorded immediately after the start of CO<sub>2</sub> flow, with absorption reaching 465.4 mg/g at 2160 min. Following the CO<sub>2</sub> cutoff, a gradual desorption was observed; however, the rate of desorption was notably lower than that of pure water, and the return to initial mass was delayed.

The behavior shown in Fig. 7 demonstrates the catalytic effect of carbonic anhydrase in accelerating the conversion of CO<sub>2</sub> into bicarbonate in aqueous environments. In pure water, the absorption of CO<sub>2</sub> is governed by the slow, uncatalyzed hydration of CO<sub>2</sub> molecules, a reversible equilibrium process. Once CO<sub>2</sub> supply ceases, the dissolved CO<sub>2</sub> is released back into the atmosphere due to the absence of solid-phase sinks or reactive ions to stabilize it.

With the enzyme present, the reaction kinetics change significantly. Carbonic anhydrase catalyzes the reversible hydration of CO<sub>2</sub> ( $\text{CO}_2 + \text{H}_2\text{O} \rightleftharpoons \text{HCO}_3^- + \text{H}^+$ ), leading to a rapid buildup of bicarbonate ions in solution. This not only enhances the initial absorption rate but also increases the total amount of CO<sub>2</sub> retained during the absorption phase. Although the process remains reversible, the presence of bicarbonate in higher concentrations slows down the desorption rate.

However, because water lacks reactive cations (like Ca<sup>2+</sup> or Mg<sup>2+</sup>), the bicarbonate formed cannot convert into stable carbonates, and thus, no permanent sequestration occurs. This is evident from the eventual return of the enzyme solution to near its original mass, like water, albeit over a longer period. These findings underscore that while carbonic anhydrase enhances CO<sub>2</sub> hydration kinetics, permanent CO<sub>2</sub> capture requires coupling with reactive alkaline materials to form solid carbonates.

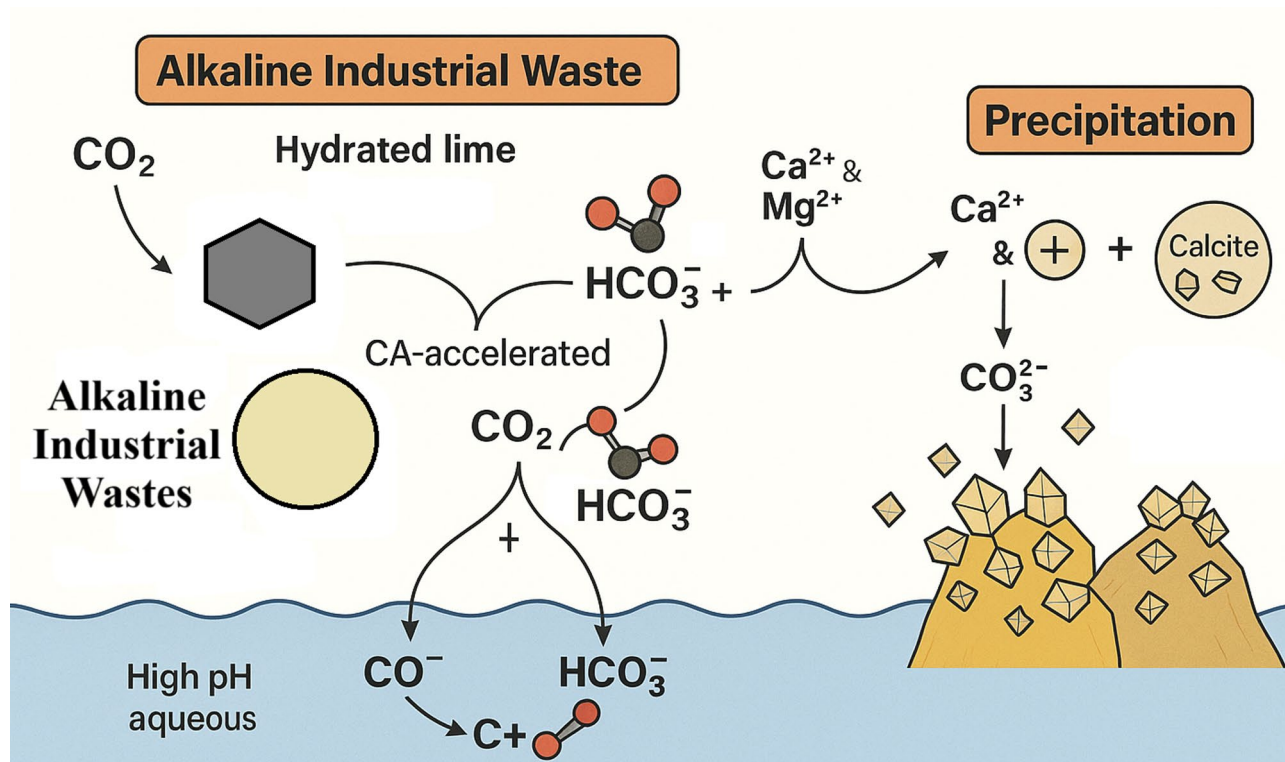


**Fig. 6.** Enzyme-enhanced CO<sub>2</sub> mineralization in alkaline industrial wastes.

Figure 8 presents the CO<sub>2</sub> absorption behavior of (a) hydrated lime and (b) cement, both with and without carbonic anhydrase enzyme. In each case, CO<sub>2</sub> gas was supplied for 1440 min and then stopped to observe desorption or stabilization trends.

In Fig. 8a, hydrated lime shows moderate CO<sub>2</sub> absorption when used alone, reaching a peak value of 131.33 mg/g at 1440 min. After the CO<sub>2</sub> cutoff, a small decrease in absorption is observed, indicating partial desorption or stabilization. However, when the enzyme was added, the absorption rate increased significantly, reaching 318.07 mg/g at 120 min and peaking at 474.13 mg/g at 1440 min. After the CO<sub>2</sub> supply ended, the weight remained mostly stable, indicating a high degree of permanent CO<sub>2</sub> fixation.

Figure 8b shows similar trends for cement. Without the enzyme, cement absorbed CO<sub>2</sub> slowly, peaking at 55.47 mg/g, and remaining flat after that. The addition of the enzyme led to a substantial enhancement in both the rate and extent of absorption, with a maximum of 285.93 mg/g by 1440 min. Post-cutoff, the mass plateaued with no notable desorption, suggesting stable carbonate formation.

The results in Fig. 8 underscore the importance of both chemical reactivity and enzymatic enhancement in CO<sub>2</sub> mineralization. Hydrated lime, a highly reactive alkaline material rich in Ca(OH)<sub>2</sub>, readily reacts with CO<sub>2</sub> to form CaCO<sub>3</sub>. In the presence of carbonic anhydrase, the hydration of CO<sub>2</sub> to bicarbonate is greatly accelerated, increasing the local concentration of reactive intermediates. This, in turn, facilitates faster and more extensive precipitation of carbonate phases. The near-stable mass after CO<sub>2</sub> cutoff in both cases, particularly with the enzyme, confirms the formation of solid carbonates and minimal reversibility of the process.

Cement, on the other hand, contains residual Ca(OH)<sub>2</sub> and other partially hydrated phases, making its reactivity slower and more complex. The enzyme's role in this matrix is to boost the hydration of CO<sub>2</sub> so that it can efficiently react with the limited available Ca<sup>2+</sup>. As seen in the cement + enzyme case, the absorption increased more than fivefold compared to the untreated cement. The enzyme thus acts as a kinetic enhancer, particularly beneficial in materials with moderate to low baseline reactivity.

### CO<sub>2</sub> absorption in complex industrial byproducts

Figure 9 illustrates the CO<sub>2</sub> absorption behavior of (a) fly ash and (b) slag, comparing samples with and without the addition of carbonic anhydrase enzyme. CO<sub>2</sub> gas was supplied for 360 min, followed by a shutdown phase to observe retention or desorption trends.

In Fig. 9a, the untreated fly ash exhibited a gradual increase in CO<sub>2</sub> uptake, reaching 85.66 mg/g at 360 min. After the CO<sub>2</sub> supply was stopped, the sample displayed a progressive decrease in absorption, indicating partial CO<sub>2</sub> desorption. In contrast, the enzyme-enhanced fly ash showed a sharp initial rise in absorption, peaking at 308.27 mg/g at 360 min. After the cutoff, the curve remained mostly stable, indicating successful CO<sub>2</sub> retention.

Figure 9b shows similar trends for slag. The untreated slag reached a maximum of 86.67 mg/g at 360 min, with a relatively flat absorption curve thereafter. The slag treated with the enzyme exhibited a much steeper absorption trajectory, achieving 312.27 mg/g by 360 min, with little change after CO<sub>2</sub> cutoff.

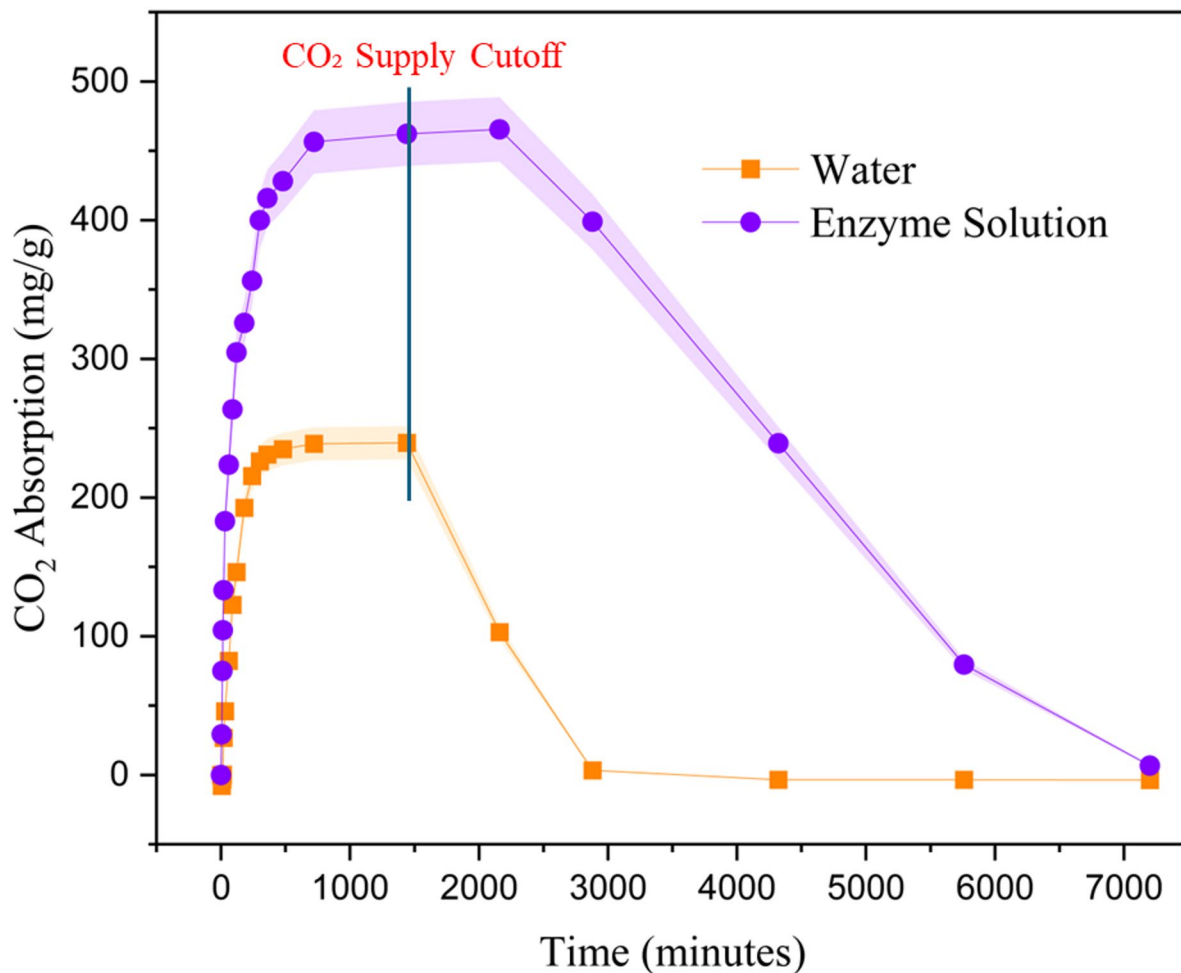


Fig. 7. CO<sub>2</sub> absorption in water and enzyme solution.

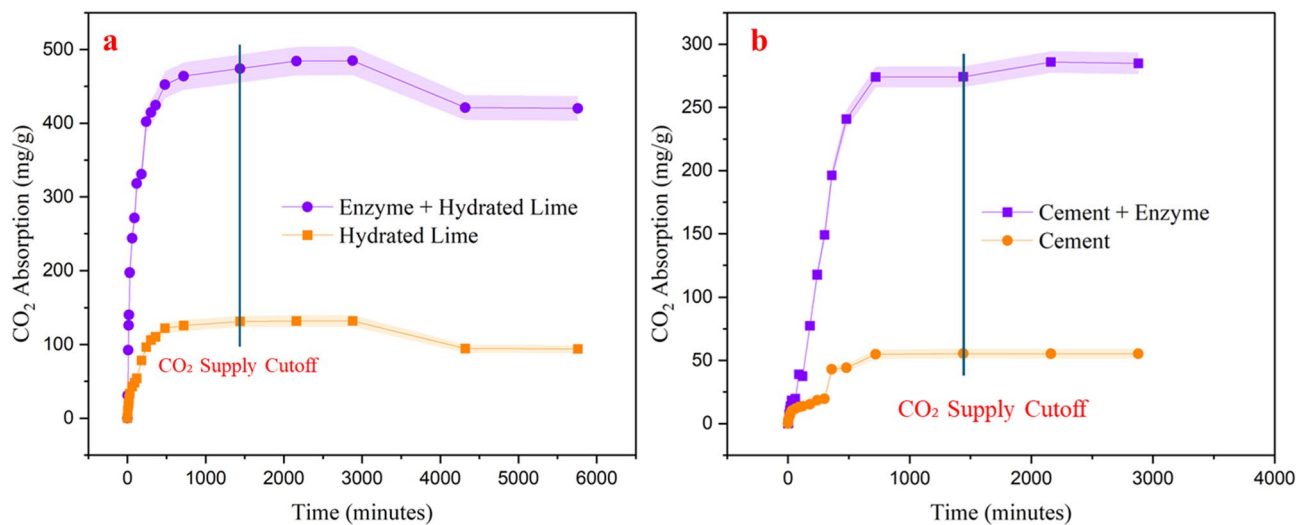
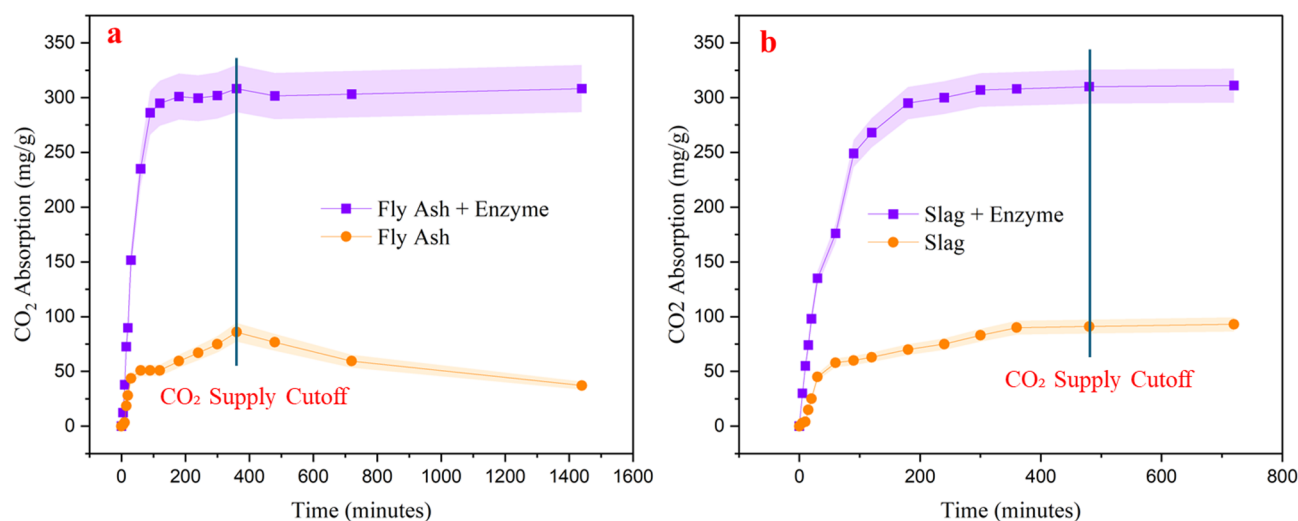


Fig. 8. CO<sub>2</sub> absorption behavior of (a) hydrated lime with and without CA and (b) cement with and without CA.



**Fig. 9.** CO<sub>2</sub> absorption performance of (a) fly ash with and without CA and (b) slag with and without CA.

The results in Fig. 9 highlight the distinct behaviors of two industrial by-products, fly ash and slag, in CO<sub>2</sub> capture scenarios, especially when catalyzed by carbonic anhydrase. Fly ash, composed primarily of amorphous aluminosilicate glass with minor reactive phases, typically releases Ca<sup>2+</sup>, Mg<sup>2+</sup>, and other metal ions at a slower rate. The enzyme's role here is crucial: by accelerating CO<sub>2</sub> hydration to bicarbonate, it enhances the opportunity for bicarbonate ions to react with the slowly released metal cations, forming insoluble carbonates. This mechanism accounts for the observed improvement in both absorption rate and retention in enzyme-enhanced fly ash samples. The post-cutoff plateau confirms that a significant portion of CO<sub>2</sub> was mineralized and retained.

For slag, a material with a higher baseline reactivity due to its content of CaO, MgO, and silicate phases, the CO<sub>2</sub> absorption behavior mirrors that of fly ash but occurs more efficiently even without the enzyme. However, enzyme addition results in a markedly higher final absorption value. The rapid increase and plateau observed post-cutoff indicate that the system approached mineral carbonation saturation quickly. The catalytic action of carbonic anhydrase ensured a sufficient supply of bicarbonate for reactions with divalent metal cations, leading to stable carbonate formation.

In both materials, the minimal or negligible desorption after CO<sub>2</sub> cutoff in enzyme-treated samples provides compelling evidence of permanent CO<sub>2</sub> sequestration via mineralization pathways. The enzyme does not store CO<sub>2</sub> but significantly accelerates the formation of carbonate precipitates through enhanced bicarbonate availability.

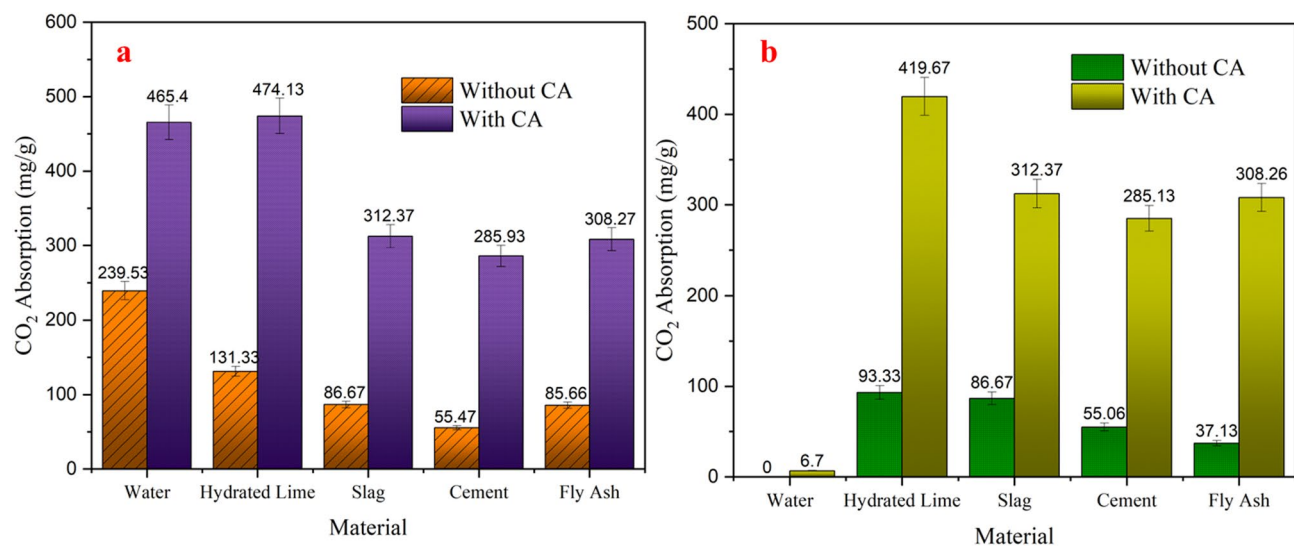
### Comparison of the effects of enzyme on CO<sub>2</sub> absorption

Figure 10a shows the comparison of peak absorption values of CO<sub>2</sub> across all different materials used in this study. For alkaline materials tested in this study, the rank of these materials in terms of peak CO<sub>2</sub> absorption is: hydrated lime > fly ash > slag > cement. This is possibly due to the constituents of mineral components in these materials. The figure shows that with the enzyme; all these materials showed a significant increase in peak CO<sub>2</sub> absorption. With the use of enzyme, the CO<sub>2</sub> absorption by water increased from 239.53 mg/g to 465.4 mg/g; the CO<sub>2</sub> absorption by hydrated lime increased from 131.33 mg/g to 474.13 mg/g; the absorption in slag increased from 86.67 mg/g to 312.37 mg/g; the CO<sub>2</sub> absorption by cement increased from 55.47 mg/g to 285.93 mg/g; and the CO<sub>2</sub> absorption by fly ash increased from 85.66 mg/g to 308.27 mg/g. The possible mechanism is that the enzyme accelerates the CO<sub>2</sub> dissolution into water, which accelerates the formation of carbonates and bicarbonates, resulting in higher CO<sub>2</sub> absorption efficiency.

With the depressure of CO<sub>2</sub>, a portion of the dissolved CO<sub>2</sub> was released. What remained was the CO<sub>2</sub> that was permanently fixed by carbonated minerals such as calcite. Figure 10b summarizes the amount of CO<sub>2</sub> that was permanently absorbed by different materials. The figure shows that the use of the enzyme increased the permanent absorption capacity of all alkaline materials. In the case of pure water, it absorbed a good amount of CO<sub>2</sub>, but all of the CO<sub>2</sub> was released back into the atmosphere when the CO<sub>2</sub> supply was cut off, leading to zero permanent absorption. When the enzyme was added to the water, it showed a similar trend with a negligible permanent absorption of 6.7 mg/g. This indicates that water has a very limited or no capacity to permanently sequester CO<sub>2</sub>.

In contrast, the impact of the enzyme on industrial materials such as hydrated lime, slag, cement, and fly ash is more pronounced. Hydrated lime permanently sequestered 93.33 mg/g of CO<sub>2</sub>, and with the enzyme, this value rose significantly to 419.667 mg/g. A comparable trend was observed in all other materials, where the presence of the enzyme notably enhanced their ability to permanently absorb CO<sub>2</sub>. In the case of slag, absorption increased from 86.67 mg/g to 312.37 mg/g. In cement, it rose from 55.067 mg/g to 285.133 mg/g, and for fly ash, it increased from 37.133 mg/g to 308.2667 mg/g.

The data shown in Figs. 10a and b confirm the catalytic role of carbonic anhydrase (CA) in enhancing the kinetics of CO<sub>2</sub> absorption and mineralization across various alkaline materials. Rather than increasing the



**Fig. 10.** (a) Comparison of maximum CO<sub>2</sub> absorption (mg/g) across different materials with and without carbonic anhydrase (b) Comparison of permanent CO<sub>2</sub> absorption (mg/g) measured after CO<sub>2</sub> supply cutoff.

inherent CO<sub>2</sub> storage capacity of these materials, the enzyme accelerates the hydration of CO<sub>2</sub> to bicarbonate, thereby enabling faster reaction with available alkaline cations such as Ca<sup>2+</sup> or Mg<sup>2+</sup> within the timeframe of the experiment.

Across all enzyme-treated samples, a significantly higher percentage of the absorbed CO<sub>2</sub> was permanently fixed compared to their untreated samples. For example, in hydrated lime, the percentage of permanent CO<sub>2</sub> absorption rose from approximately 71% without enzyme to nearly 89% with enzyme. In fly ash, this shift was even more pronounced, increasing from about 43% to almost 100%. These results highlight how enzyme presence enables the material to utilize more of its reactive potential within a limited reaction window.

In materials such as cement and slag, which naturally showed high retention rates even without the enzyme, the enzyme allowed for faster completion of mineralization reactions. This did not change the final proportion of CO<sub>2</sub> fixed but significantly increased the amount captured during the same period, indicating that the enzyme helped the system reach its equilibrium state more rapidly. This supports the enzyme's role as a kinetic enhancer, not a sequestration agent.

Water, by contrast, demonstrated the boundary of enzyme utility. Even with CA, only a small fraction of the absorbed CO<sub>2</sub> was retained, confirming that without mineral cations to react with bicarbonate, the enzyme cannot support permanent CO<sub>2</sub> capture.

These patterns support the conclusion that CA enhances CO<sub>2</sub> fixation rates during the active gas-solids reaction period, without influencing the final equilibrium or acting as a sink itself. The permanent capture observed in enzyme-treated systems occurred because more CO<sub>2</sub> was successfully mineralized within the limited experimental duration, not because the enzyme altered the chemical endpoint of the system.

### Reusability of enzyme

To assess the reusability of the enzyme, repetitive experiments were conducted by using hydrated lime. After a complete round of CO<sub>2</sub> absorption test with hydrated lime and enzyme, the bicarbonates were allowed to settle down. The enzyme solution above the solid sediment layer was carefully extracted. The recycled liquid was then used for another round of CO<sub>2</sub> absorption test using a new batch of hydrated lime only. The same procedure for the recycling of enzymic liquid was repeated for additional CO<sub>2</sub> absorption cycles with hydrated lime. Figure 11 summarizes the absorption behaviors for all these absorption cycles. The results showed a consistent trend of CO<sub>2</sub> absorption with only slight decreases in the peak amount of CO<sub>2</sub> absorption. The slight reduction might partially be attributed to the loss of a portion of the enzyme during the extraction process. The reuse of the enzyme still maintained a significant 87.9% of CO<sub>2</sub> absorption at cycle 4. The experimental observations suggest that the enzyme retains most of its catalytic activity. The slight decrease in the CO<sub>2</sub> absorption over the reuse cycles is possibly due to a minor loss during the extraction of the enzyme solution at the end of testing. The reuse of enzyme presents a promising approach to reducing the cost of enzyme.

### Statistical analysis of enzyme impact on CO<sub>2</sub> absorption

To quantitatively assess the significance of the observed enhancements in CO<sub>2</sub> absorption due to the addition of carbonic anhydrase, a statistical analysis was conducted across all tested industrial byproducts: hydrated lime, fly ash, and slag.

Each absorption experiment was performed in triplicate (n=3), and the final CO<sub>2</sub> uptake values (mg/g) at 720 min were used for comparison. The data were first tested for normality and homogeneity of variances using the Shapiro–Wilk and Levene's tests, respectively. Based on these assumptions, both one-way ANOVA and

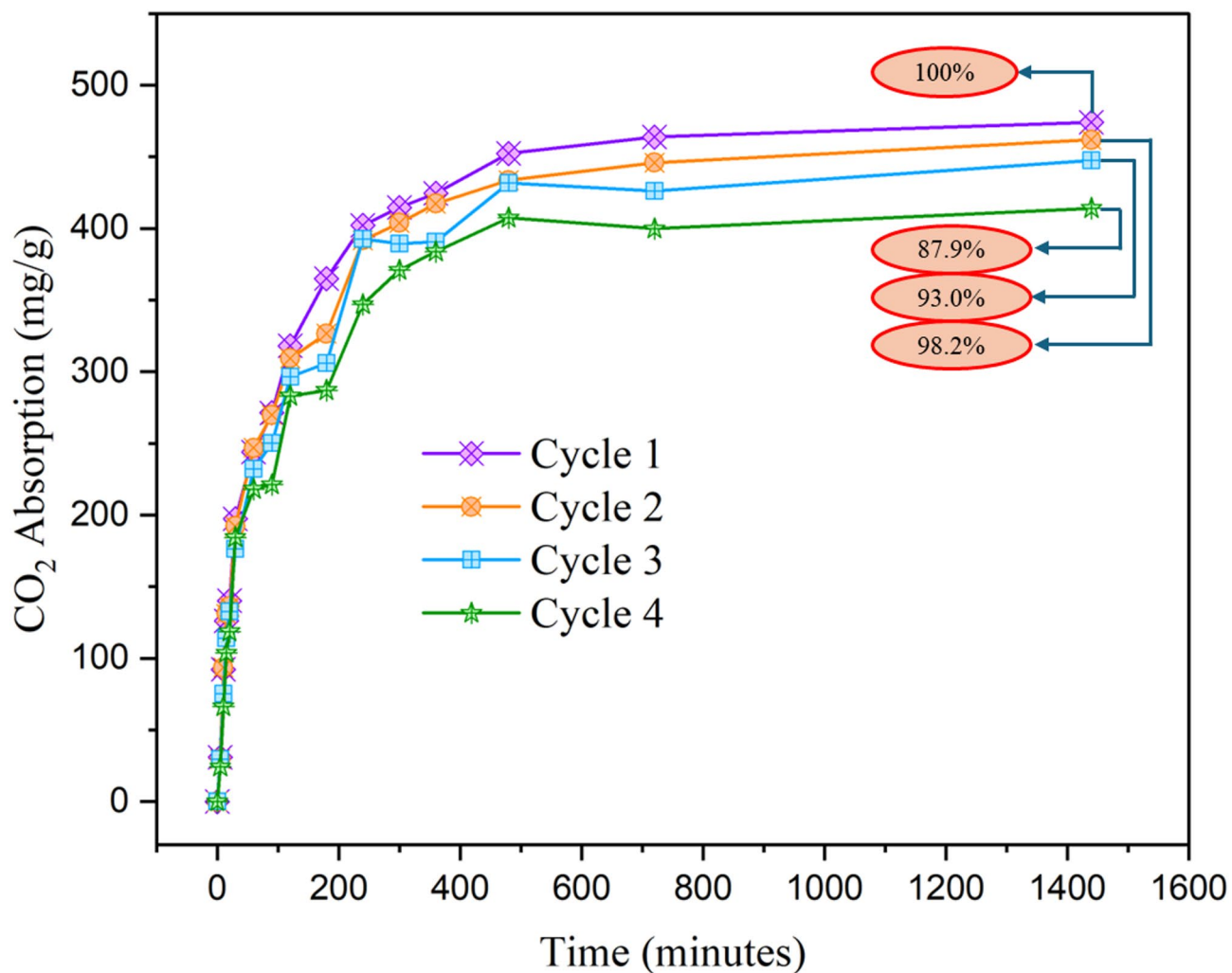


**Fig. 11.** CO<sub>2</sub> absorption behaviors by reuse of the enzyme over different testing cycles.

Material	Condition	Mean CO <sub>2</sub> Uptake (mg/g)	Std. Dev	<i>p</i> -value (t-test)
Hydrated lime	Without enzyme	421.3	6.2	0.0007
	With enzyme	474.1	5.7	
Fly ash	Without enzyme	392.0	7.1	0.0021
	With enzyme	440.7	6.4	
Slag	Without enzyme	353.2	5.8	0.0014
	With enzyme	416.8	4.9	

**Table 1.** Statistical analysis of CO<sub>2</sub> uptake with and without carbonic anhydrase.

independent two-sample t-tests were employed to evaluate statistical differences between enzyme-assisted and control groups.

The ANOVA results showed a significant overall effect of enzyme addition on CO<sub>2</sub> absorption across all material types ( $p < 0.01$ ). To further validate these findings, two-sample t-tests were performed between the enzyme and control groups for each material individually. The following mean  $\pm$  standard deviation values and *p*-values were obtained as shown in Table 1.

The low *p*-values ( $p < 0.005$ ) across all materials confirm that the enzyme-assisted systems achieved statistically significant increases in CO<sub>2</sub> absorption. These enhancements are attributed to the accelerated formation of bicarbonate ions catalyzed by CA, which improves the availability of carbonate species for subsequent mineralization with Ca<sup>2+</sup> from the solid phase.

All statistical analyses were conducted using Python, and a significance level of  $\alpha = 0.05$  was used throughout.

## Discussion

The results show that carbonic anhydrase (CA) consistently increases both the total CO<sub>2</sub> absorbed during flow and the fraction retained as solid carbonates after cutoff across hydrated lime, cement, fly ash, and slag. The enhancement is most pronounced for hydrated lime and measurable for cement, fly ash, and slag, reflecting how readily each material supplies divalent cations for carbonate precipitation. The permanence observed after the gas is turned off indicates that the added mass is not simply dissolved CO<sub>2</sub> but mineralized products, predominantly CaCO<sub>3</sub>, formed on the particle surfaces. These outcomes align with prior reports that CA accelerates the hydration step and thereby raises local carbonate availability without changing the thermodynamic endpoint of mineralization<sup>40–42</sup>.

Although the enzyme is intrinsically fast, the apparent reaction rate in our suspensions is limited by processes that are not enzyme-controlled. Gas–liquid transfer of CO<sub>2</sub> into a particle-laden boundary layer, diffusion through that layer, and the dissolution of Ca- or Mg-bearing phases to supply cations all slow the overall sequence. Once a carbonate shell forms on reactive surfaces, further growth requires ion transport through the newly formed product, which introduces an additional diffusion barrier and explains the gradual approach to a plateau. Similar transitions from an initial chemically controlled stage to a diffusion-limited stage are well documented for mineral carbonation systems and were reproduced here under ambient conditions. Thus, the “slow enzyme kinetics” observed at the reactor scale arises from mass-transfer and solid-state constraints rather than from low catalytic turnover of CA itself<sup>43–46</sup>.

Material composition strongly modulates both the magnitude of the CA benefit and the overall rate. Hydrated lime, dominated by Ca(OH)<sub>2</sub>, releases Ca<sup>2+</sup> rapidly and supports fast nucleation and growth of CaCO<sub>3</sub>; cement behaves similarly due to residual portlandite after hydration, albeit with slower release within a more complex matrix. Fly ash and slag contain substantial SiO<sub>2</sub> and Al<sub>2</sub>O<sub>3</sub> and more limited free CaO or MgO, so cation release is slower, and the CA advantage manifests primarily as faster attainment of the same thermodynamic endpoint<sup>47,48</sup>. Trace metals and aluminosilicate surfaces can also interact with the enzyme; literature notes that multivalent cations and certain surfaces can partially inhibit or adsorb CA, which would further dampen apparent activity in ash and slag systems. Even with these interactions, the enzyme retained most of its activity over four reuse cycles, indicating that reversible transport and surface effects dominate over irreversible enzyme deactivation in our conditions.

Taken together, the data support a surface-coupled mechanism in which CA increases bicarbonate/carbonate generation within the thin liquid film at particle interfaces, boosting local supersaturation and promoting heterogeneous nucleation on lime, cement, ash, and slag. The subsequent slowdown is consistent with armoring or passivation by newly precipitated carbonates and with limited replenishment of Ca<sup>2+</sup>/Mg<sup>2+</sup> from the solid. These interpretations are consistent with microscopy-based observations reported for carbonation of lime-based binders and industrial residues, where product layers gradually reduce access to reactive cores. From an application standpoint, this implies that engineering the microenvironment around the enzyme and the solid, by increasing effective interfacial area, refreshing surfaces, or moderating product-layer growth, should yield the largest practical gains<sup>31,49</sup>.

The reusability tests indicate that homogeneous CA can be recycled with only modest loss of performance across cycles, which is encouraging for cost and process design. Nonetheless, industrial deployment would benefit from enzyme immobilization or entrapment strategies that stabilize CA against adsorption, shear, and ionic effects while enabling easy recovery; such approaches have shown improved operational stability in gas–liquid contactors and slurry systems. Buffer-layer engineering or local co-solutes that preserve the catalytic Zn<sup>2+</sup> environment may further mitigate transient inhibition by dissolved metals common in ash and slag leachates<sup>50–52</sup>.

## Conclusions

This study shows the potential of carbonic anhydrase to enhance the carbon dioxide capture capabilities of various alkaline industrial materials, including lime, cement, fly ash, and slag. The experimental findings show that the presence of CA significantly increased both the rate of CO<sub>2</sub> absorption and the proportion of CO<sub>2</sub> that was permanently sequestered as stable carbonate minerals within the reaction timeframe. This improvement is attributed to the enzyme's catalytic role, which accelerates the conversion of CO<sub>2</sub> into bicarbonate, thereby enabling more rapid reaction with available cations such as calcium and magnesium.

The enzyme does not alter the thermodynamic equilibrium of the reaction but instead allows the system to reach equilibrium faster. As a result, materials that would otherwise absorb CO<sub>2</sub> slowly or only partially can more effectively sequester carbon when the enzyme is present.

The reusability tests further support the viability of this approach, as CA retained most of its catalytic activity over multiple absorption cycles. This stability highlights the enzyme's potential for use in scalable and economically feasible carbon capture applications. By combining industrial alkaline byproducts with enzymatic catalysis, this approach offers a sustainable pathway to utilize existing waste materials for CO<sub>2</sub> capture.

The integration of carbonic anhydrase into CO<sub>2</sub> capture systems could contribute significantly to climate change mitigation efforts, especially when applied to construction and industrial processes where such materials are already widely used. Continued research into enzyme stabilization, immobilization, and long-term performance will be essential to transition this approach from lab-scale demonstrations to practical, real-world applications targeted at supporting global carbon neutrality goals. Future work should focus on enhancing enzyme durability under alkaline conditions by exploring strategies such as developing alkali-resistant CA mutants or immobilizing enzymes on stable carrier materials to prolong their activity and recyclability in industrial applications.

## Data availability

The datasets generated and/or analysed during the current study are not publicly available due to the research in progress but are available from the corresponding author on reasonable request.

Received: 11 August 2025; Accepted: 22 December 2025

Published online: 09 January 2026

## References

1. Talekar, S., Jo, B. H., Dordick, J. S. & Kim, J. Carbonic anhydrase for CO<sub>2</sub> capture, conversion and utilization. *Curr. Opin. Biotechnol.* <https://doi.org/10.1016/j.copbio.2021.12.003> (2022).
2. Vaz, S., Rodrigues de Souza, A. P. & Lobo Baeta, B. E. Technologies for carbon dioxide capture: A review applied to energy sectors. *Clean. Eng. Technol.* **8**, 100456. <https://doi.org/10.1016/j.clet.2022.100456> (2022).
3. Gür, T. M. Carbon dioxide emissions, capture, storage and utilization: review of materials, processes and technologies. *Prog. Energy Combust. Sci.* **89**, 100965. <https://doi.org/10.1016/j.pecs.2021.100965> (2022).
4. Rasouli, H., Nguyen, K. & Iliuta, M. C. Recent advancements in carbonic anhydrase immobilization and its implementation in CO<sub>2</sub> capture technologies: A review. *Sep. Purif. Technol.* **296**, 121299. <https://doi.org/10.1016/j.seppur.2022.121299> (2022).
5. Molina-Fernández, C. & Luis, P. Immobilization of carbonic anhydrase for CO<sub>2</sub> capture and its industrial implementation: A review. *J. CO<sub>2</sub> Util.* **47**, 101475 (2021).
6. International energy Agency, I. Global Status Report Towards a Zero-Emission, Efficient and Resilient Buildings and Construction Sector (2018).
7. Global Status Report for Buildings and Construction 2024/25 Not Just Another Brick in the Wall.
8. Cao, T. N. D. et al. Unraveling the potential of electrochemical pH-swing processes for carbon dioxide capture and utilization. *Ind. Eng. Chem. Res.* **62**, 20979–20995. <https://doi.org/10.1021/acs.iecr.3c02183> (2023).
9. La Plante, E. C. et al. Electrolytic seawater mineralization and the mass balances that demonstrate carbon dioxide removal. *ACS EST Eng.* **3**, 955–968 (2023).
10. Wang, Q., Cao, Z., Li, Q. & Song, B. Advances in concurrent CO<sub>2</sub> sequestration and heavy metal mobilization during fly ash carbonation: A review. *Carbon Capture Sci. Technol.* **17**, 100519. <https://doi.org/10.1016/j.cst.2025.100519> (2025).
11. Abdalla, M. & Wang, Q. Carbon mineralization and lithium extraction in phyllosilicates under different temperatures and CO<sub>2</sub> pressures: Advancing secure CO<sub>2</sub> storage and utilization strategies. *Energy Fuels* **39**, 11211–11228 (2025).
12. Li, N., Mo, L. & Unluer, C. Emerging CO<sub>2</sub> utilization technologies for construction materials: A review. *J. CO<sub>2</sub> Util.* **65**, 102237. <https://doi.org/10.1016/j.jcou.2022.102237> (2022).
13. Waleed, M., Liaqat, N., Jamil, M.A.-B., Khalid, R. A. & Jamil, S. M. Unconfined compressive strength and freeze-thaw behavior of silty clay soils treated with bio-enzyme. *Arab. J. Geosci.* **16**, 275 (2023).
14. Alissandratos, A. & Easton, C. J. Biocatalysis for the application of CO<sub>2</sub> as a chemical feedstock. *Beilstein J. Org. Chem.* **11**, 2370–2387. <https://doi.org/10.3762/bjoc.11.259> (2015).
15. Chaudhury, S. R., Sharma, U., Thapliyal, P. C. & Singh, L. P. Low-CO<sub>2</sub> emission strategies to achieve net zero target in cement sector. *J. Clean. Prod.* **417**, 137466. <https://doi.org/10.1016/j.jclepro.2023.137466> (2023).
16. Yong, J. K. J., Stevens, G. W., Caruso, F. & Kentish, S. E. The use of carbonic anhydrase to accelerate carbon dioxide capture processes. *J. Chem. Technol. Biotechnol.* **90**, 3–10 (2015).
17. Oyewole, K. A., Okedere, O. B., Rabi, K. O., Alawode, K. O. & Oyelami, S. Carbon dioxide emission, mitigation and storage technologies pathways. *Sustain. Environ.* **9**, 2188760. <https://doi.org/10.1080/27658511.2023.2188760> (2023).
18. Jaitak, A., Kumari, K., Kounder, S. & Monga, V. Carbonic anhydrases: Moiety appended derivatives, medicinal and pharmacological implications. *Bioorg. Med. Chem.* **114**, 117933. <https://doi.org/10.1016/j.bmc.2024.117933> (2024).
19. Alterio, V. et al. Zeta-carbonic anhydrases show CS<sub>2</sub> hydrolase activity: A new metabolic carbon acquisition pathway in diatoms?. *Comput. Struct. Biotechnol. J.* **19**, 3427–3436 (2021).
20. Xu, Y., Lin, Y., Chew, N. G. P., Malde, C. & Wang, R. Biocatalytic PVDF composite hollow fiber membranes for CO<sub>2</sub> removal in gas-liquid membrane contactor. *J. Memb. Sci.* **572**, 532–544 (2019).
21. Lindskog, S. *Structure and Mechanism of Carbonic Anhydrase*. vol. 74 (1997).
22. Ayaz Khan, M. N. et al. Effect of Brick Dust on Strength and Workability of Concrete. in *IOP Conference Series: Materials Science and Engineering* vol. 414 (Institute of Physics Publishing, 2018).
23. de Oliveira Maciel, A., Christakopoulos, P., Rova, U. & Antonopoulou, I. Carbonic anhydrase to boost CO<sub>2</sub> sequestration: Improving carbon capture utilization and storage (CCUS). *Chemosphere* **299**, 134419. <https://doi.org/10.1016/j.chemosphere.2022.134419> (2022).
24. Mondal, M., Khanra, S., Tiwari, O. N., Gayen, K. & Halder, G. N. Role of carbonic anhydrase on the way to biological carbon capture through microalgae—A mini review. *Environ. Prog. Sustain. Energy* **35**, 1605–1615. <https://doi.org/10.1002/ep.12394> (2016).
25. Bong, G. M. et al. Development of integrated system for biomimetic CO<sub>2</sub> sequestration using the enzyme carbonic anhydrase. *Energy Fuels* **15**, 309–316 (2001).
26. Energy Agency, I. *Energy Technology Perspectives 2020*. [www.iea.org/t&c/](http://www.iea.org/t&c/).
27. Liaqat, N., Farjad Sami, M., Umer, M., Manan, A. & Umar, M. Potential of Lime for Stabilization of Subgrade Soil of Gujranwala Region. <http://www.ijser.org> (2019).
28. Liaqat, N. et al. Influence of RHA on Engineering Properties of Medium Plastic Clay. [www.ijert.org](http://www.ijert.org).
29. Villa, R., Nieto, S., Donaire, A. & Lozano, P. Direct biocatalytic processes for CO<sub>2</sub> capture as a green tool to produce value-added chemicals. *Molecules* **28**, 5520. <https://doi.org/10.3390/molecules28145520> (2023).
30. Sharma, A. et al. Carbonic anhydrase robustness for use in nanoscale CO<sub>2</sub> capture technologies. *ACS Omega* **8**, 37830–37841 (2023).
31. Ruiz-Agudo, C. & Cölfen, H. Exploring the potential of nonclassical crystallization pathways to advance cementitious materials. *Chem. Rev.* **124**, 7538–7618. <https://doi.org/10.1021/acs.chemrev.3c00259> (2024).
32. Rodríguez-Navarro, C., Ilić, T., Ruiz-Agudo, E. & Elert, K. Carbonation mechanisms and kinetics of lime-based binders: An overview. *Cement and Concr. Res.* **173**, 107301. <https://doi.org/10.1016/j.cemconres.2023.107301> (2023).
33. Zhang, S., Zhang, Z., Lu, Y., Rostam-Abadi, M. & Jones, A. Activity and stability of immobilized carbonic anhydrase for promoting CO<sub>2</sub> absorption into a carbonate solution for post-combustion CO<sub>2</sub> capture. *Bioresour Technol.* **102**, 10194–10201 (2011).
34. Xv, J. et al. Accelerated CO<sub>2</sub> capture using immobilized carbonic anhydrase on polyethyleneimine/dopamine co-deposited MOFs. *Biochem. Eng. J.* **189**, 108719 (2022).
35. Xie, Y. et al. Recent applications of carbonic anhydrase and its mimics in CO<sub>2</sub> capture and utilization technologies. *Geoenergy Sci. Eng.* **252**, 213958. <https://doi.org/10.1016/j.geoen.2025.213958> (2025).
36. *Activation and Startup Time*.
37. Air-Oxygen-Mass-Flow-Meter.
38. PSP145.
39. DS\_PM\_0012\_Revise9.

40. Hazarika, A. & Yadav, M. Biomineralization of carbon dioxide by carbonic anhydrase. *Biocatal. Agric. Biotechnol.* **51**, 102755. <https://doi.org/10.1016/j.bcab.2023.102755> (2023).
41. Rodriguez-Navarro, C. et al. The multiple roles of carbonic anhydrase in calcium carbonate mineralization. *CrystEngComm* **21**, 7407–7423 (2019).
42. Gadikota, G. Carbon mineralization pathways for carbon capture, storage and utilization. *Commun. Chem.* **4**, 23. <https://doi.org/10.1038/s42004-021-00461-x> (2021).
43. Zong, J. & Yue, J. Continuous solid particle flow in microreactors for efficient chemical conversion. *Ind. Eng. Chem. Res.* **61**, 6269–6291. <https://doi.org/10.1021/acs.iecr.2c00473> (2022).
44. Stewart, M. P., Langer, R. & Jensen, K. F. Intracellular delivery by membrane disruption: Mechanisms, strategies, and concepts. *Chem. Rev.* **118**, 7409–7531. <https://doi.org/10.1021/acs.chemrev.7b00678> (2018).
45. Xie, F., Gao, C. & Avérous, L. Alginate-based materials: Enhancing properties through multiphase formulation design and processing innovation. *Mater. Sci. Eng. R: Rep.* **159**, 100799. <https://doi.org/10.1016/j.mser.2024.100799> (2024).
46. Lavrentev, F. V. et al. Diffusion-limited processes in hydrogels with chosen applications from drug delivery to electronic components. *Molecules* <https://doi.org/10.3390/molecules28155931> (2023).
47. Control of crystallization pressure in cementitious materials using a bio-based inhibitor.
48. Kellermeier, M. et al. Von Ionen zu Kristallen: Neue Einblicke die nicht-klassische Keimbildung von Calciumsulfat. *Angew. Chem.* **136**, e202408429 (2024).
49. Rodriguez-Navarro, C., Ilić, T., Ruiz-Agudo, E. & Elert, K. Carbonation mechanisms and kinetics of lime-based binders: An overview. *Cement Concr. Res.* **173**, 107301. <https://doi.org/10.1016/j.cemconres.2023.107301> (2023).
50. Tadesse, M. & Liu, Y. Recent advances in enzyme immobilization: The role of artificial intelligence, novel nanomaterials, and dynamic carrier systems. *Catalysts* **15**, 571. <https://doi.org/10.3390/catal15060571> (2025).
51. Maghraby, Y. R., El-Shabasy, R. M., Ibrahim, A. H. & Azzazy, H. M. E. S. Enzyme immobilization technologies and industrial applications. *ACS Omega* **8**, 5184–5196. <https://doi.org/10.1021/acsomega.2c07560> (2023).
52. Robescu, M. S. & Bavaro, T. A comprehensive guide to enzyme immobilization: All you need to know. *Molecules* **30**, 939. <https://doi.org/10.3390/molecules30040939> (2025).

## Acknowledgements

We appreciate the help of Diego Franco Ocampo, Department Engineer, and Jim Berilla, Department Technician, for their help with this research. The work is partially supported by the US Department of Energy (DE-SC0025232).

## Author contributions

X.Y.: designed and directed this project, improved the methodology, and revised the manuscript. N.L.: design and implement the research, analyze experimental data, and write the manuscript.

## Declarations

## Competing interests

The authors declare no competing interests.

## Additional information

**Correspondence** and requests for materials should be addressed to X.B.Y.

**Reprints and permissions information** is available at [www.nature.com/reprints](http://www.nature.com/reprints).

**Publisher's note** Springer Nature remains neutral with regard to jurisdictional claims in published maps and institutional affiliations.

**Open Access** This article is licensed under a Creative Commons Attribution-NonCommercial-NoDerivatives 4.0 International License, which permits any non-commercial use, sharing, distribution and reproduction in any medium or format, as long as you give appropriate credit to the original author(s) and the source, provide a link to the Creative Commons licence, and indicate if you modified the licensed material. You do not have permission under this licence to share adapted material derived from this article or parts of it. The images or other third party material in this article are included in the article's Creative Commons licence, unless indicated otherwise in a credit line to the material. If material is not included in the article's Creative Commons licence and your intended use is not permitted by statutory regulation or exceeds the permitted use, you will need to obtain permission directly from the copyright holder. To view a copy of this licence, visit <http://creativecommons.org/licenses/by-nc-nd/4.0/>.

© The Author(s) 2025